ENHANCING QUADCOPTER CONTROL: A MODEL REFERENCE ADAPTIVE CONTROL APPROACH WITH NEURAL NETWORKS

Salvatore Rosario Bassolillo¹, Gennaro Raspaolo², Luciano Blasi² & Egidio D'Amato¹

 $^1\mathrm{Department}$ of Science and Technology, University of Naples Parthenope, 80143, Napoli, Italy

Abstract

In recent decades, multirotor flying vehicles have garnered significant attention due to their diverse configurations and versatility. This paper focuses on the design and testing of a flight control scheme employing Model Reference Adaptive Control with Neural Networks. The effectiveness of the proposed controller is demonstrated through numerical simulations on a detailed nonlinear simulator.

Keywords: UAV, quadcopter, MRAC, adaptive control

1. General Introduction

In a rapidly evolving landscape, unmanned aerial vehicles (UAVs), commonly known as drones, have greatly expanded their operational capabilities, proving invaluable in military and civil applications. This paper delves into the civilian use of micro and mini UAVs for tasks such as aerial photography, mapping, weather forecasting, and more. The focus is on multirotor UAVs, particularly quadrotors, which offer a balance of low cost and structural simplicity [1, 2]. Furthermore, their ability to take-off and land vertically, fly in confined spaces and hover over a specified area offers considerable advantages when used for missions in hazardous environments [3].

Despite the advantages and the possibility of adopting reliable onboard trajectory planners [4, 5, 6], highly non-linear dynamics and the presence of atmospheric disturbances make the control of multirotors a very challenging problem. Over the years, both linear and non-linear control systems have been adopted to stabilize quadrotors [7]. Conventional control methods are based on Proportional-Integral-Derivative (PID) controllers [8, 9] because of their ease of implementation. These controllers are well suited for applications in quasi-steady conditions, where the model dynamics can be linearized [10]. However, quadrotors exhibit a strong nonlinear behavior in most practical applications, such as in the presence of wind gusts or aggressive maneuvers, and PID controllers fail to converge. To overcome these difficulties, more adaptive and nonlinear control strategies have been adopted by researcher, such as Adaptive Control [11], Model Reference Adaptive Control [12, 13, 14], Dynamic Inversion Control [15], Linear Quadratic Regulators (LQR) [16, 17], Model Predictive Control [18, 19], H_{inf} Control [20, 21, 22], and Neural Networks [23], just to mention some examples. This paper introduces a groundbreaking quadcopter configuration employing a Model Reference Adaptive Control (MRAC) system integrated with Neural Networks. This innovative design enhances flight control precision and adaptability to varying mission requirements.

The proposed quadcopter design leverages MRAC [24, 25] with Neural Networks, addressing the complexities associated with control redundancy, non-linear dynamics and uncertainties. In order to achieve the desired performance of the quadrotor, the MRAC control technique is able to automatically adjust the parameters of the control model in real-time when the plant parameters are unknown or change during operations [26]. In [14], the authors proposed a control architecture based on MRAC capable of enabling trajectory tracking for quadcopters, despite uncertainties about the inertial properties of the aircraft and the presence of unknown and unsteady payloads. The authors in [13]

²Department of Engineering, University of Campania Luigi Vanvitelli, 81031, Aversa (CE), Italy

leveraged the features of MRAC to develop a controller for a built-in quadcopter, able to autonomously adapt control parameters to various operational scenarios different from the reference model without any external intervention from the pilot. Embedding Neural Networks enhances adaptability, allowing for efficient and reliable control amidst changing conditions [27]. For an easy adaptation to changing environments, a quadrotor position controller based on Neural Network trained used Reinforcement Learning technique was presented in [23]. To effectively address problems related to parametric uncertainties and external disturbance, the authors in [28] combine the neural network adaptive scheme with sliding mode control for the position and attitude tracking control of a quadrotor UAV.

The presented two-level flight control strategy consists of an outer loop ensuring precise altitude control, while an inner loop focuses on attitude control [29, 30]. The MRAC system, coupled with Neural Networks, facilitates adaptive learning and optimization, ensuring optimal performance in different scenarios.

The paper presents results by means of numerical simulations, incorporating uncertainties and measurement noise, to validate the effectiveness of the proposed controller.

The paper is organized as follows: Section 2. introduces the adopted aircraft model. Section 3. describes the proposed flight control algorithm. Finally, to assess the performance of the proposed strategy, Section 3 presents the results of the numerical simulation analysis.

2. Aircraft model

The motion of the aircraft can be defined by employing the rigid body dynamic equations and two reference frames: an inertial earth-fixed frame denoted as E, and a body-fixed frame denoted as B, with its origin O_B located at the Center of Gravity (CG) of the vehicle.

Consider a rigid body whose state is defined as $\mathbf{X} = [\mathbf{V}^T, \mathbf{\Omega}^T, \mathbf{\Theta}^T, \mathbf{z}^T]^T$, where \mathbf{V} denotes the velocity vector in the body reference frame, $\mathbf{\Omega} = [\omega_x, \omega_y, \omega_z]^T$ stands for the vector of angular rates in the Body frame. Additionally, $\mathbf{\Theta}$ symbolizes the vector of attitude descriptors, Euler angles ϕ , θ , ψ or quaternions described subsequently, and the vector $\mathbf{z} = [x_E, y_E, z_E]^T$ denotes the vehicle position in the earth-fixed frame E.

The equations governing the dynamic model of the UAV in the body-fixed frame *B* can subsequently be expressed as:

$$m(\dot{\mathbf{V}} + \mathbf{\Omega} \times \mathbf{V}) = \mathbf{F}(\mathbf{V}, \mathbf{\Omega}, \mathbf{\Theta}, \mathbf{u})$$
(1)

$$\mathbf{J}\dot{\mathbf{\Omega}} + \mathbf{B}(\mathbf{\Omega})\mathbf{J}\mathbf{\Omega} = \mathbf{T}(\mathbf{V}, \mathbf{\Omega}, \mathbf{u}) \tag{2}$$

$$\dot{\mathbf{z}} = \mathbf{R}_{BE}^{-1}(\mathbf{\Theta})\mathbf{V} \tag{3}$$

$$\dot{\Theta} = \mathbf{H}(\Theta)\Omega \tag{4}$$

where m is the mass of the quadrotor, whereas $\dot{\mathbf{V}}$ represents the time derivative of the vector \mathbf{V} as observed in the body frame. \mathbf{F} is the vector of external forces, a function of both motion variables and the vector \mathbf{u} representing propellers rotational speed used for vehicle control, and $\mathbf{J} = \text{diag}(I_{xx}, I_{yy}, I_{zz})$ represents the inertia matrix, assumed diagonal and constant in the Body frame. The vector \mathbf{T} stands for the applied moments with respect to the Center of Gravity (CG), and \mathbf{R}_{BE} denotes the rotation matrix from the earth-fixed frame to the body frame, dependent on attitude. The skew-symmetric matrix $\mathbf{B}(\Omega)$ is employed to express the external product between Ω and $\mathbf{J}\Omega$.

$$B(\Omega) = \begin{pmatrix} 0 & -\omega_z & \omega_y \\ \omega_z & 0 & -\omega_x \\ -\omega_y & \omega_x & 0 \end{pmatrix}$$
 (5)

The external forces and moments in (1) and (2) can be deconstructed into distinct components as follows:

$$F(V, \Omega, \Theta, \mathbf{u}) = F_{\mathbf{g}}(\Theta) + F_{\mathbf{p}}(V, \Omega, \mathbf{u}) + F_{\mathbf{a}}(V, \Omega)$$
(6)

$$T(V,\Omega,u) = T_p(V,\Omega,u) + T_a(V,\Omega)$$
(7)

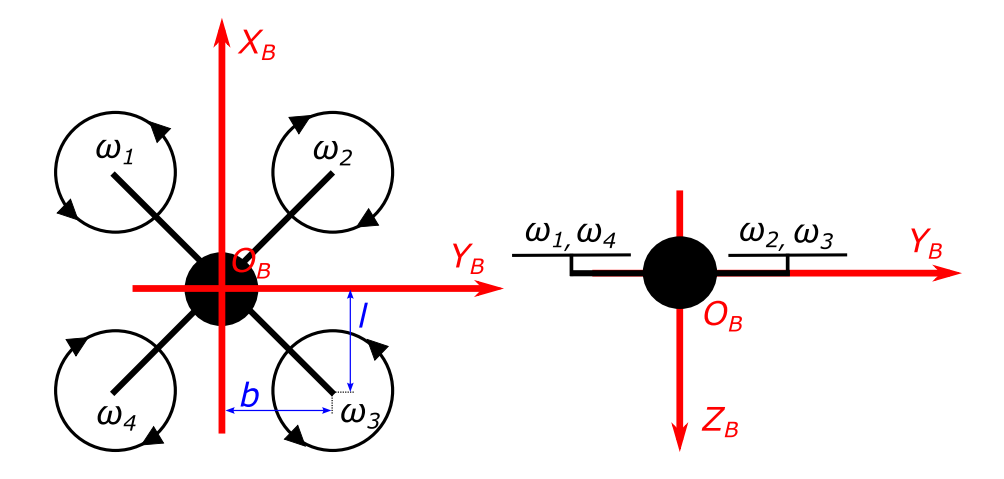


Figure 1 – Quadrotor configuration and Body reference frame.

Here, $\mathbf{F_g} = \mathbf{R}_{BE}[0,0,mg]^T$ denotes the gravitational force, $\mathbf{F_p}$ and $\mathbf{T_p}$ represent the propulsive forces and moments, whereas $\mathbf{F_a}$ and $\mathbf{T_a}$ are the aerodynamic forces and moments, respectively. As for $\mathbf{F_p} = [F_{px}, F_{py}, F_{pz}]^T$ and $\mathbf{T_p} = [L_p, M_p, N_p]^T$, neglecting F_{px} and F_{py} , the remaining components can be expressed as a combination of forces F_i and torques T_i acting on the four propellers (i = 1, 2, 3, 4). These forces and torques are modeled as quadratic functions of rotor speeds ω_i :

$$F_i = k_f(\omega_i)\omega_i^2 T_i = k_t(\omega_i)\omega_i^2 \forall i = 1, 2, 3, 4$$
(8)

Here, k_f and k_t denote force and torque coefficients, mainly dependent on the rotational speed at lower values of the vehicle speed. These coefficients have been determined through experimental tests.

Considering a quadcopter in cross-configuration (see Figure 1), the propulsive force component F_{pz} , as well as the moments L_p , M_p , and N_p in the body reference frame, exhibit a relationship with control inputs, as expressed by:

$$\begin{bmatrix} F_{pz} \\ L_p \\ M_p \\ N_p \end{bmatrix} = \begin{bmatrix} k_f & k_f & k_f & k_f \\ bk_f & -bk_f & -bk_f & bk_f \\ lk_f & lk_f & -lk_f & -lk_f \\ k_t & -k_t & k_t & -k_t \end{bmatrix} \begin{bmatrix} \omega_1^2 \\ \omega_2^2 \\ \omega_3^2 \\ \omega_4^2 \end{bmatrix}$$
(9)

The parameters b and l denote the distance of the rotors center from CG along the y and x axes, respectively.

In the context where rotor speeds can be regarded as control inputs, assuming the actuator time response is significantly faster than the closed-loop system dynamics, a static nonlinear relationship is required. This relationship maps control inputs to Pulse Width Modulation (PWM) signals governing brushless motors and servos and must be implemented on board.

3. Flight Control Algorithm

The quadrotor can be operated in either an automatic or semi-automatic mode. In the Semi-Automatic Control Mode (SACM), the quadrotor acts as a Remotely Piloted Vehicle (RPV), with the pilot supplying attitude reference signals and total thrust to the onboard flight control system. In the Automatic Control Mode (ACM), the Ground Control Station (GCS) provides reference positions or waypoints in the earth-fixed reference frame, while the onboard control system ensures path following through these waypoints.

The Flight Control System (FCS) consists of three primary components (see Figure 2):

• A Control Allocator (CA), responsible for distributing the control effort (requested forces and moments) among available effectors (control of propeller rotational speeds).

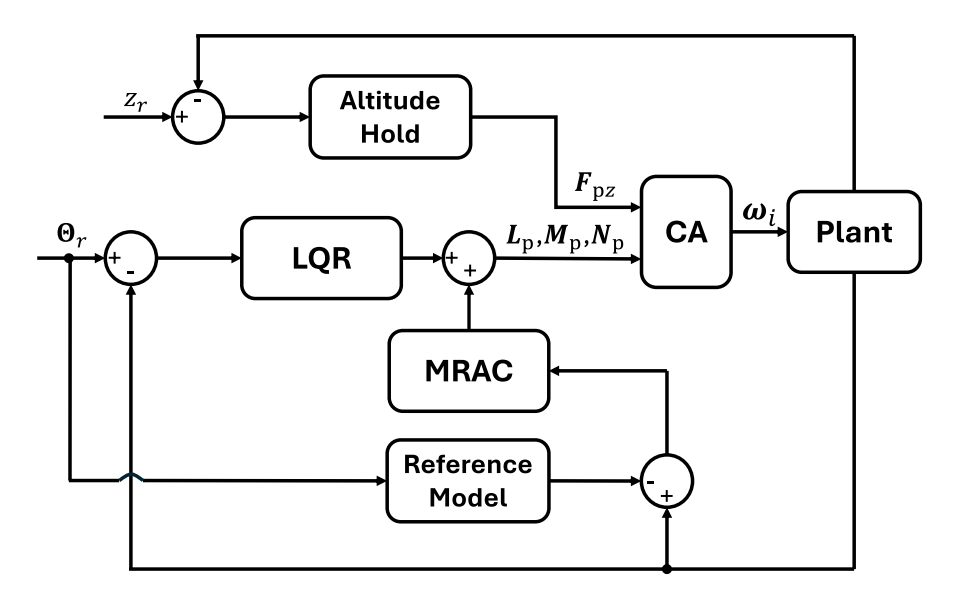


Figure 2 – General scheme of the Flight Control System.

- An internal loop for attitude control, characterized by fast dynamics, yielding virtual requested moments to the Control Allocator through an LQR and an MRAC controller to compensate for any nonlinearities.
- An external loop for altitude control, characterized by slow dynamics, generating virtual force commands to the Control Allocator.

3.1 Control Allocator

Virtual forces and moments given in input to the system need to be translated into real input commands for the quadcopter actuator. The Control Allocator provides the proper input commands to the quadrotor as represented in Eq. 10.

$$\begin{bmatrix} \omega_{1}^{2} \\ \omega_{2}^{2} \\ \omega_{3}^{2} \\ \omega_{4}^{2} \end{bmatrix} = \begin{bmatrix} \frac{1}{4k_{f}} & \frac{1}{4bk_{f}} & \frac{1}{4lk_{f}} & \frac{1}{4k_{i}} \\ \frac{1}{4k_{f}} & -\frac{1}{4bk_{f}} & \frac{1}{4lk_{f}} & -\frac{1}{4k_{i}} \\ \frac{1}{4k_{f}} & -\frac{1}{4bk_{f}} & -\frac{1}{4lk_{f}} & \frac{1}{4k_{i}} \\ \frac{1}{4k_{f}} & \frac{1}{4bk_{f}} & -\frac{1}{4lk_{f}} & -\frac{1}{4k_{i}} \\ \end{bmatrix} \begin{bmatrix} F_{pz} \\ L_{p} \\ M_{p} \\ N_{p} \end{bmatrix}$$
(10)

3.2 Inner Loop Control

The inner loop control allows stabilizing the attitude of the quadrotor through the combination of a baseline LQR model and an adaptive controller based on MRAC.

LQR controllers are widely used in aerospace applications for their characteristics of stability, robustness, and optimality, as well as their easy applicability for the control of MIMO systems, especially for attitude control problems of quadcopter [31].

Let us consider the linear system defined by Eq. (11).

$$\dot{\mathbf{x}}(t) = \mathbf{A}\mathbf{x}(t) + \mathbf{B}\mathbf{u}(t) \tag{11}$$

where $\mathbf{x} = [\mathbf{\Omega}^T, \mathbf{\Theta}^T]^T \in \mathbb{R}^m$ is a reduced state vector for attitude control purposes, $\mathbf{u} \in \mathbb{R}^n$ is the control input, $\mathbf{A} \in \mathbb{R}^{mxm}$ and $\mathbf{B} \in \mathbb{R}^{mxn}$ are unknown constant matrices.

The LQR controller considers the feedback state control law, shown by Eq. (12), to minimize the cost function defined by Eq (13).

$$\mathbf{u}_{LOR}(t) = -K * \mathbf{x} \tag{12}$$

$$J(\mathbf{x}, \mathbf{u}) = \int_0^\infty [\mathbf{x}^T(t)\mathbf{Q}\mathbf{x}(t) + \mathbf{u}^T(t)\mathbf{R}\mathbf{u}(t)] dt$$
 (13)

The optimal control gain, K, can be evaluated using Eq. (14), where **P** is found by solving the Riccati Equation, defined by Eq. (15).

$$K = \mathbf{R}^{-1} \mathbf{B}^T \mathbf{P} \tag{14}$$

$$\mathbf{A}^{T}\mathbf{P} + \mathbf{P}\mathbf{A} + \mathbf{Q} - \mathbf{P}\mathbf{B}\mathbf{R}^{-1}\mathbf{B}^{T}\mathbf{P} = \mathbf{0}$$
(15)

Despite the robustness characteristics of the LQR, the emergence of nonlinearities, associated, for example, with structural damages or engine failures, leads to a deterioration in the performance of the controller [32]. In this regard, coupling an MRAC to LQR controller allows compensating for such nonlinearities, effectively stabilizing the attitude of the quadrotor. Indeed, the main aim of the MRAC control block is to adjust the control parameters in real time so that the output of the plant tracks the output of a reference model with the same reference input.

To account for modeling errors or system control failures, let us introduce uncertainties into the model described in Eq. (11). This way, the set of equations describing the state dynamics is modified in accordance with Eq. (16).

$$\dot{\mathbf{x}}(t) = \mathbf{A}\mathbf{x}(t) + \mathbf{B}\mathbf{\Lambda} \left(\mathbf{u}(t) + \mathbf{f}(\mathbf{X})\right) \tag{16}$$

The matrix Λ is a diagonal matrix to account for potential uncertainties in control system effectiveness, whose elements are strictly positive.

Since the model shown in Eq. (11) is a linear approximation of a nonlinear system that is valid in a small region around a particular flight condition, the non-linear function $\mathbf{f}(\mathbf{X}) = [\mathbf{f_F}(\mathbf{X})^T, \mathbf{f_T}(\mathbf{X})^T]^T$ allows for accounting for system uncertainties and disturbances that may arise from flight conditions different from those considered during linearization. In this regard, the components of $\mathbf{f}(\mathbf{X})$ can be defined according to Eqs. (17) and (18).

$$\mathbf{f}_{\mathbf{F}}(\mathbf{X}) = \mathbf{F}_{\mathbf{a}}(\mathbf{V}, \mathbf{\Omega}) + \mathbf{F}_{\mathbf{p}}(\mathbf{V}, \mathbf{\Omega}) \tag{17}$$

$$\mathbf{f}_{\mathbf{T}}(\mathbf{X}) = \mathbf{T}_{\mathbf{a}}(\mathbf{V}, \mathbf{\Omega}) + \mathbf{T}_{\mathbf{p}}(\mathbf{V}, \mathbf{\Omega}) \tag{18}$$

The aerodynamic components F_a and T_a take into account uncertainties related to the incomplete aerodynamic model for flight conditions different from the hovering phase, while the components F_p and T_p consider the uncertainty in identifying actuator characteristics and any disturbances related to a loss of actuator performance.

The designed adaptive control law must be able to ensure that the system defined in Eq. (16) can track the state \mathbf{x}_r of a given reference plant model, as defined in Eq. (19), thus ensuring a desired behavior, even in the presence of disturbances and uncertainties.

$$\dot{\mathbf{x}}_r(t) = \mathbf{A}_r \mathbf{x}_r(t) + \mathbf{B}_r \mathbf{r}(t) \tag{19}$$

The matrix $\mathbf{A}_r \in \mathbb{R}^{mxm}$ is a stable matrix, $\mathbf{B}_r \in \mathbb{R}^{mxn}$, and $\mathbf{r}(t) \in \mathbb{R}^n$ is the reference input vector. Considering a neural network with a single layer of N hidden neurons, the MRAC controller computes the control input according to Eq. (20).

$$\mathbf{u}_{MRAC}(t) = -\mathbf{w}(t)^T \Phi(\mathbf{x}) \tag{20}$$

 $\Phi(\mathbf{x}) = [\Phi_1(\mathbf{x}), \Phi_2(\mathbf{x}), ..., \Phi_N(\mathbf{x})]^T$ represents the vector of Radial Basis Functions, whereas $\mathbf{w}(t) \in \mathbb{R}^{n \times N}$ is the hidden layer weights matrix ([33]).

To update $\mathbf{w}(t)$ (Eq. (22)), the controller evaluates the tracking error between the states of the controlled system and the states of the reference model (Eq. (21)).

$$\mathbf{e}(t) = \mathbf{x}(t) - \mathbf{x}_r(t) \tag{21}$$

$$\dot{\mathbf{w}}(t) = -\Gamma(\Phi \mathbf{e}^T \mathbb{P} \mathbf{B} - \sigma \mathbf{w}) \tag{22}$$

Table 1 – Quadcopter main characteristics.

	Value
m [kg]	0.5
l $[m]$	0.2
b $[m]$	0.2
$\mathbf{J} [kg * m^2]$	$diag(5*10^{-3}, 5*10^{-3}, 1*10^{-2})$

The parameter Γ represents the rates of adaptation of the weight vector terms, σ ensures that the weights remain bounded without needing persistent excitation ([34, 27]), and \mathbb{P} is the solution of the Lyapunov equation [33].

The total amount of the attitude control provided to the plant is a combination of the control inputs from LQR and MRAC as defined in Eq. (23).

$$\mathbf{u}_{\Theta}(t) = \mathbf{u}_{LOR}(t) + \mathbf{u}_{MRAC}(t) \tag{23}$$

3.3 Outer Loop Control

The outer loop control block, based on a PID controller [35], provides the appropriate control effort, in terms of requested force, F_{pz} , to the CA block for tracking a reference altitude, z_r .

4. Numerical Results

The proposed flight control scheme was tested on a comprehensive quadrotor simulator implemented in Matlab-Simulink environment.

Considering the relatively low dynamic pressure and the absence of lifting surfaces in near-hovering conditions, at this stage of the control system design phase, both aerodynamic forces and moments have been omitted.

The main quadcopter characteristics are summarized in Table 1.

To assess the controller robustness, additional model uncertainties were considered. In particular, we added a CG position deviation of 0.02m along the x-axis, introducing an unbalance moment around the pitch axis, and a 20% variation of the vehicle inertia matrix data. Furthermore, numerical simulations also take into account first-order linear actuator dynamics with saturations and the presence of measurement noise observed during flights.

To highlight the performance of the proposed controller, a sequence of two distinct attitude maneuvers around body axis was selected. In particular, two rectangular signals with a duration of 5s each and amplitudes of 0.2rad and 0.1rad were considered as inputs for the roll, pitch, and yaw channels.

As can be seen in Figures 3a and 3c, control systems with and without MRAC are equally effective in response to the roll and yaw input signals, both able to compensate model uncertainties introduced in terms of variation of the inertia matrix data. On the other hand, once a further model uncertainty is added in terms of CG position deviation along the x-axis, a significant bias appears in the response of LQR pitch attitude controller (see Figure 3b). In this case, the MRAC control action allows to effectively compensate for this bias, providing satisfactory results in the system response. In particular, the proposed control system architecture, combining LQR and MRAC controllers, is able to assure a tracking error compliant with the accuracy of the low-cost Inertial Measurement Units (IMUs) typically involved in this kind of air vehicle.

5. Conclusions

In this paper, the design and testing of a flight control scheme based on MRAC with Neural Networks is presented. The effectiveness of the proposed control algorithm has been tested through numerical simulations on a nonlinear quadcopter simulator, performing a sequence of maneuvers around body axes in the presence of non-modeled dynamics. Model uncertainties have been added in terms of CG position deviation, introducing an unbalance moment around the pitch axis, and variation of the vehicle inertia matrix data. A comparison of results with and without the MRAC compensator showed that the combined use of LQR and MRAC controllers provides the best performance in the presence

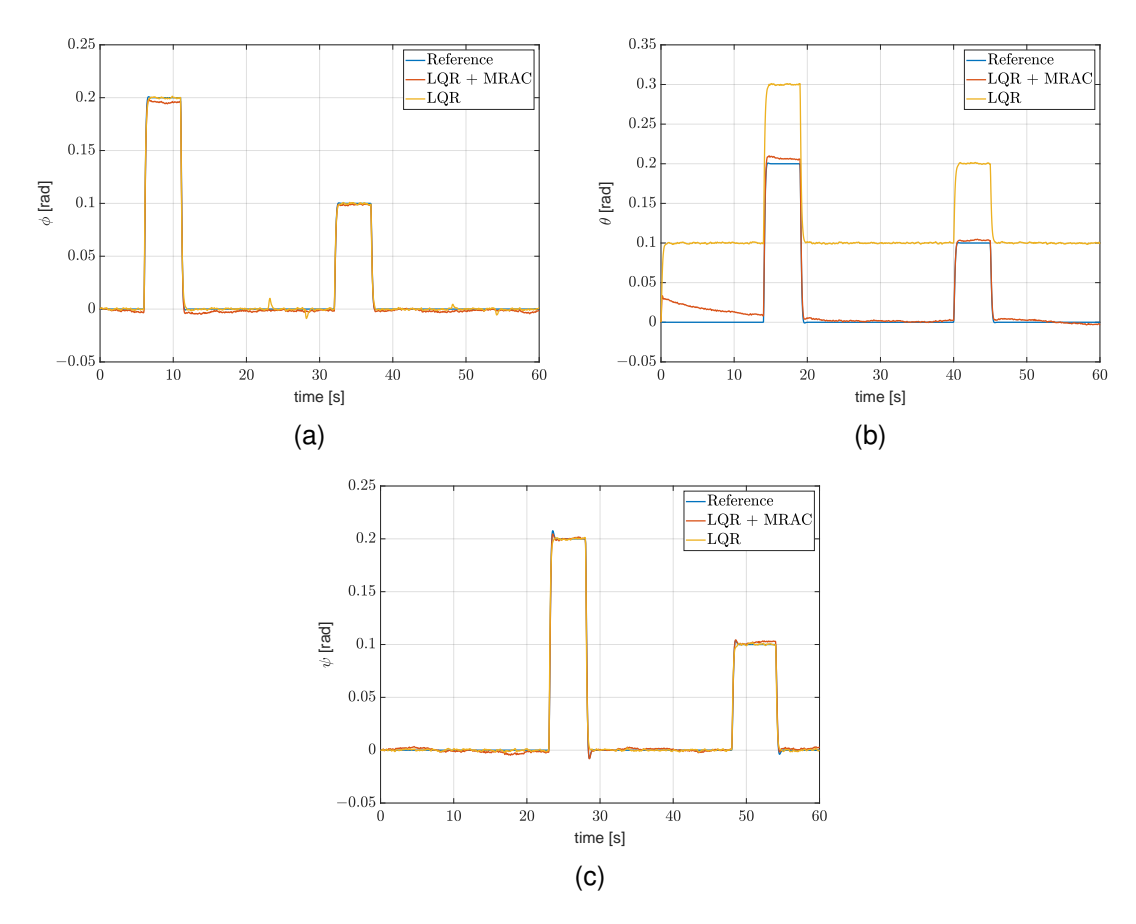


Figure 3 – Numerical simulation results on roll (a), pitch (b), and yaw (c) channel, with and without MRAC controller.

of model uncertainties, namely when these concern the CG position. In particular, the proposed control system architecture was able to ensure limited tracking errors, avoiding the excessive bias shown in the response of the pitch attitude controller without the use of MRAC. As future work, the proposed control algorithm will be implemented on a real model, allowing to assess its performance through a dedicated campaign of experimental tests in indoor laboratories with the assistance of a flight arena.

6. Contact Author Email Address

For any further information, mail to: salvatorerosario.bassolillo@collaboratore.uniparthenope.it

7. Copyright Statement

The authors confirm that they, and/or their company or organization, hold copyright on all of the original material included in this paper. The authors also confirm that they have obtained permission, from the copyright holder of any third party material included in this paper, to publish it as part of their paper. The authors confirm that they give permission, or have obtained permission from the copyright holder of this paper, for the publication and distribution of this paper as part of the ICAS proceedings or as individual off-prints from the proceedings.

8. Acknowledgement

This work was supported by the research project - ID:20222N4C8E "Resilient and Secure Networked Multive-hicle Systems in Adversary Environments" granted by the Italian Ministry of University and Research (MUR) within the PRIN 2022 program, funded by the European Union through the PNRR program.









References

- [1] G. Muchiri and S. Kimathi, "A review of applications and potential applications of uav," in *Proceedings of the Sustainable Research and Innovation Conference*, pp. 280–283, 2022.
- [2] P. Pannozzi, K. P. Valavanis, M. J. Rutherford, G. Guglieri, M. Scanavino, and F. Quagliotti, "Urban monitoring of smart communities using uas," in *2019 International Conference on Unmanned Aircraft Systems (ICUAS)*, pp. 866–873, IEEE, 2019.
- [3] A. Jaimes, S. Kota, and J. Gomez, "An approach to surveillance an area using swarm of fixed wing and quad-rotor unmanned aerial vehicles uav (s)," in 2008 IEEE International Conference on System of Systems Engineering, pp. 1–6, IEEE, 2008.
- [4] V. A. Nardi, A. Ferraro, and V. Scordamaglia, "Feasible trajectory planning algorithm for a skid-steered tracked mobile robot subject to skid and slip phenomena," in *2018 23rd International Conference on Methods & Models in Automation & Robotics (MMAR)*, pp. 120–125, IEEE, 2018.
- [5] V. Scordamaglia, V. A. Nardi, and A. Ferraro, "A feasible trajectory planning algorithm for a network controlled robot subject to skid and slip phenomena," in *2019 24th IEEE International Conference on Emerging Technologies and Factory Automation (ETFA)*, pp. 933–940, IEEE, 2019.
- [6] V. Scordamaglia and V. A. Nardi, "A set-based trajectory planning algorithm for a network controlled skid-steered tracked mobile robot subject to skid and slip phenomena," *Journal of Intelligent & Robotic Systems*, vol. 101, no. 1, p. 15, 2021.
- [7] M. Idrissi, M. Salami, and F. Annaz, "A review of quadrotor unmanned aerial vehicles: applications, architectural design and control algorithms," *Journal of Intelligent & Robotic Systems*, vol. 104, no. 2, p. 22, 2022.
- [8] H. Lim, J. Park, D. Lee, and H. J. Kim, "Build your own quadrotor: Open-source projects on unmanned aerial vehicles," *IEEE Robotics & Automation Magazine*, vol. 19, no. 3, pp. 33–45, 2012.
- [9] Q. Jiao, J. Liu, Y. Zhang, and W. Lian, "Analysis and design the controller for quadrotors based on pid control method," in *2018 33rd youth academic annual conference of Chinese association of automation (YAC)*, pp. 88–92, IEEE, 2018.
- [10] H. Liu, X. Hou, J. Kim, and Y. Zhong, "Decoupled robust velocity control for uncertain quadrotors," *Asian Journal of Control*, vol. 17, no. 1, pp. 225–233, 2015.
- [11] M. C. P. Santos, C. D. Rosales, J. A. Sarapura, M. Sarcinelli-Filho, and R. Carelli, "An adaptive dynamic controller for quadrotor to perform trajectory tracking tasks," *Journal of Intelligent & Robotic Systems*, vol. 93, pp. 5–16, 2019.
- [12] B. Whitehead and S. Bieniawski, "Model reference adaptive control of a quadrotor uav," in *AIAA Guidance, Navigation, and Control Conference*, p. 8148, 2010.
- [13] E. A. Niit and W. J. Smit, "Integration of model reference adaptive control (mrac) with px4 firmware for quadcopters," in 2017 24th International Conference on Mechatronics and Machine Vision in Practice (M2VIP), pp. 1–6, IEEE, 2017.
- [14] R. B. Anderson, J. A. Marshall, and A. L'Afflitto, "Constrained robust model reference adaptive control of a tilt-rotor quadcopter pulling an unmodeled cart," *IEEE Transactions on Aerospace and Electronic Systems*, vol. 57, no. 1, pp. 39–54, 2020.
- [15] H. Das, K. Sridhar, and R. Padhi, "Bio-inspired landing of quadrotor using improved state estimation," *IFAC-PapersOnLine*, vol. 51, no. 1, pp. 462–467, 2018.
- [16] Z. Shulong, A. Honglei, Z. Daibing, and S. Lincheng, "A new feedback linearization lqr control for attitude of quadrotor," in *2014 13th International Conference on Control Automation Robotics & Vision (ICARCV)*, pp. 1593–1597, IEEE, 2014.
- [17] S. Khatoon, D. Gupta, and L. Das, "Pid & Iqr control for a quadrotor: Modeling and simulation," in *2014 international conference on advances in computing, communications and informatics (ICACCI)*, pp. 796–802, IEEE, 2014.
- [18] M. Bangura and R. Mahony, "Real-time model predictive control for quadrotors," *IFAC Proceedings Volumes*, vol. 47, no. 3, pp. 11773–11780, 2014.
- [19] G. Franze, M. Mattei, L. Ollio, and V. Scordamaglia, "A robust constrained model predictive control scheme for norm-bounded uncertain systems with partial state measurements," *International Journal of Robust and Nonlinear Control*, vol. 29, no. 17, pp. 6105–6125, 2019.
- [20] A. Jafar, S. Fasih-UR-Rehman, S. Fazal-UR-Rehman, N. Ahmed, and M. U. Shehzad, "A robust h control for unmanned aerial vehicle against atmospheric turbulence," in *2016 2nd International Conference on Robotics and Artificial Intelligence (ICRAI)*, pp. 1–6, IEEE, 2016.
- [21] M. Babar, S. Ali, M. Shah, R. Samar, A. Bhatti, and W. Afzal, "Robust control of uavs using h control paradigm," in 2013 IEEE 9th International Conference on Emerging Technologies (ICET), pp. 1–5, IEEE,

2013.

- [22] V. Scordamaglia, A. Sollazzo, and M. Mattei, "Fixed structure flight control design of an over-actuated aircraft in the presence of actuators with different dynamic performance," *IFAC Proceedings Volumes*, vol. 45, no. 13, pp. 127–132, 2012.
- [23] J. Hwangbo, I. Sa, R. Siegwart, and M. Hutter, "Control of a quadrotor with reinforcement learning," *IEEE Robotics and Automation Letters*, vol. 2, no. 4, pp. 2096–2103, 2017.
- [24] N. T. Nguyen and N. T. Nguyen, Model-reference adaptive control. Springer, 2018.
- [25] R. B. Anderson, J. A. Marshall, and A. L'Afflitto, "Novel model reference adaptive control laws for improved transient dynamics and guaranteed saturation constraints," *Journal of the Franklin Institute*, vol. 358, no. 12, pp. 6281–6308, 2021.
- [26] D. Lara, G. Romero, R. Ibarra, A. Sánchez, and C. Pegard, "Onboard system for flight control of a small uav," in *World Automation Congress 2012*, pp. 1–6, IEEE, 2012.
- [27] E. D'Amato, G. Tartaglione, L. Blasi, M. Mattei, et al., "Nonlinear dynamic inversion with neural networks for the flight control of a low cost tilt rotor uav," in 30th Congress of the International Council of the Aeronautical Sciences, ICAS 2016, International Council of the Aeronautical Sciences, 2016.
- [28] H. Razmi and S. Afshinfar, "Neural network-based adaptive sliding mode control design for position and attitude control of a quadrotor uav," *Aerospace Science and technology*, vol. 91, pp. 12–27, 2019.
- [29] S. Ullah, Q. Khan, A. Mehmood, S. A. M. Kirmani, and O. Mechali, "Neuro-adaptive fast integral terminal sliding mode control design with variable gain robust exact differentiator for under-actuated quadcopter uav," *ISA transactions*, vol. 120, pp. 293–304, 2022.
- [30] G. Di Francesco, M. Mattei, and E. D'Amato, "Incremental nonlinear dynamic inversion and control allocation for a tilt rotor uav," in *AIAA guidance, navigation, and control conference*, p. 0963, 2014.
- [31] M. N. Shauqee, P. Rajendran, and N. M. Suhadis, "An effective proportional-double derivative-linear quadratic regulator controller for quadcopter attitude and altitude control," *Automatika: časopis za automatiku, mjerenje, elektroniku, računarstvo i komunikacije*, vol. 62, no. 3-4, pp. 415–433, 2021.
- [32] R. G. Subramanian and V. K. Elumalai, "Robust mrac augmented baseline lqr for tracking control of 2 dof helicopter," *Robotics and Autonomous Systems*, vol. 86, pp. 70–77, 2016.
- [33] P. A. Ioannou and J. Sun, *Robust adaptive control*, vol. 1. PTR Prentice-Hall Upper Saddle River, NJ, 1996.
- [34] K. Tsakalis and P. Ioannou, "Adaptive control of linear time-varying plants," *Automatica*, vol. 23, no. 4, pp. 459–468, 1987.
- [35] M. Santos, V. Pereira, A. Ribeiro, M. Silva, M. do Carmo, V. Vidal, L. Honório, A. Cerqueira, and E. Oliveira, "Simulation and comparison between a linear and nonlinear technique applied to altitude control in quadcopters," in 2017 18th International Carpathian Control Conference (ICCC), pp. 234–239, IEEE, 2017.